Accepted Manuscript

Functionalized nanogels carrying an anticancer microRNA for glioblastoma therapy

Zohar Shatsberg, Xuejiao Zhang, Paula Ofek, Shashwat Malhotra, Adva Krivitsky, Anna Scomparin, Galia Tiram, Marcelo Calderón, Rainer Haag, Ronit Satchi-Fainaro

Please cite this article as: Zohar Shatsberg, Xuejiao Zhang, Paula Ofek, Shashwat Malhotra, Adva Krivitsky, Anna Scomparin, Galia Tiram, Marcelo Calderón, Rainer Haag, Ronit Satchi-Fainaro, Functionalized nanogels carrying an anticancer microRNA for glioblastoma therapy, *Journal of Controlled Release* (2016), doi: 10.1016/j.jconrel.2016.08.029

Functionalized nanogels carrying an anticancer microRNA for glioblastoma therapy

Zohar Shatsberg*[1], Xuejiao Zhang*[2,3], Paula Ofek[1], Shashwat Malhotra[2], Adva Krivitsky[1], Anna Scomparin[1], Galia Tiram[1], Marcelo Calderón[2], Rainer Haag[¥2] and Ronit Satchi-Fainaro[¥1]

[1]Department of Physiology and Pharmacology, Sackler School of Medicine, Tel Aviv University, Tel Aviv, Israel; [2]Institute of Chemistry and Biochemistry, Freie Universität Berlin, 14195 Berlin, Germany; [3]Key Laboratory of Pollution Ecology and Environmental Engineering, Institute of Applied Ecology, Chinese Academy of Sciences, Shenyang 110016, China.

*These authors contributed equally to this work

¥ Corresponding authors:

Prof. Ronit Satchi-Fainaro, Ph.D., Department of Physiology and Pharmacology, Sackler School of Medicine, Tel Aviv University, Ramat Aviv, Tel Aviv 69978, Israel

E-mail address: ronitsf@post.tau.ac.il (R. Satchi-Fainaro). Tel.: +972 3 640 7427; fax: +972 3 640 9113.
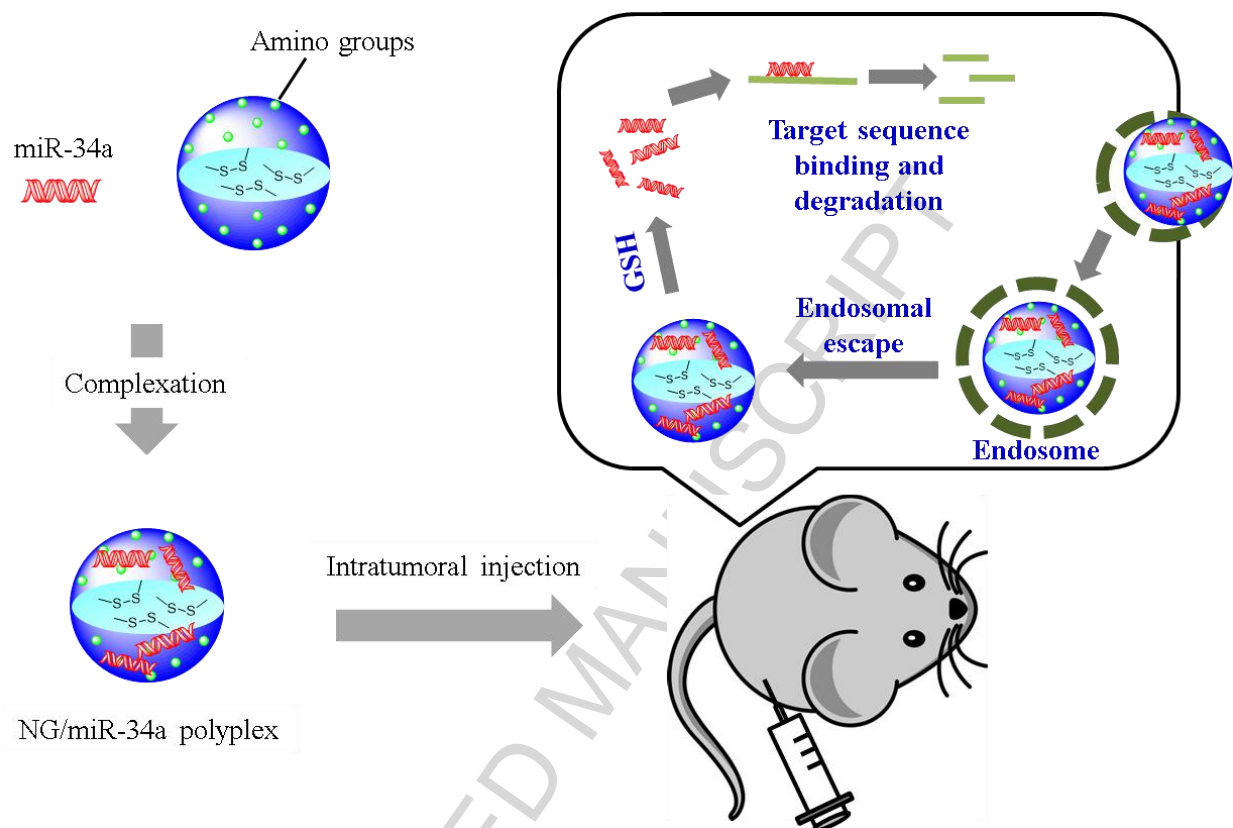
Prof. Dr. Rainer Haag, Institut für Chemie und Biochemie, Freie Universität Berlin, Takustrasse 3, 14195 Berlin, Germany

E-mail address: haag@chemie.fu-berlin.de. Tel.: +49 (30) 838 52633; Telefax: +49 (30) 838 452611

ABSTRACT

Glioblastoma Multiforme (GBM) is one of the most aggressive forms of all cancers. The median survival with current standard-of-care radiation and chemotherapy is about 14 months. GBM is difficult to treat due to heterogeneity in cancer cell population. MicroRNA-based drugs have rapidly become a vast and burgeoning field due to the ability of a microRNA (miRNA) to target many genes involved in key cellular pathways. However, *in vivo* delivery of miRNA remains a crucial challenge for its therapeutic success. To bypass this shortcoming, we designed polymeric nanogels (NGs), which are based on a polyglycerol-scaffold, as a new strategy of miRNA delivery for GBM therapy. We focused on miR-34a, which is known for its key role in important oncogenic pathways and its tumor suppression ability in GBM and other cancers. We evaluated the capability of six NG derivatives to complex with miR-34a, neutralize its negative charge and deliver active miRNA to the cell cytoplasm. Human U-87 MG GBM cells treated with our NG-miR-34a nano-polyplexes showed remarkable downregulation of miR-34a target genes, which play key roles in the regulation of apoptosis and cell cycle arrest, and induce inhibition of cells proliferation and migration. Administration of NG-miR-34a nano-polyplexes to human U-87 MG GBM-bearing SCID mice significantly inhibited tumor growth as opposed to treatment with NG-negative control miR polyplex or saline. The comparison between different polyplexes highlighted the key features for the rational design of polymeric delivery systems for oligonucleotides. Taken together, we expect that this new therapeutic approach will pave the way for safe and efficient therapies for GBM.

Graphical abstract

INTRODUCTION

MicroRNAs (miRNAs) are short noncoding RNA species, 19-24 nucleotides in length, which regulate gene expression via impaired sequence-specific base-pair hybridization to the sense mRNA [1]. As such, miRNAs can target tens to hundreds of genes and lead to inhibition of translation or mRNA degradation [2]. To date, more than 1500 human miRNAs have been annotated and found to regulate at least 20-30% of all protein-encoding genes [3, 4]. Being implicated in the control of many fundamental cellular and physiological processes, miRNAs affect numerous cancer-related signaling pathways such as differentiation, metabolism, proliferation, cell cycle control, migration and apoptosis [5]. miRNAs have been widely associated with cancer events and progression for more than a decade [6, 7]. In the last few

3

years, several reports indicated that the miR-34 family (including miR-34a, miR-34b and miR-34c) inhibits the proliferation and migration of a broad range of cancer cells, both in culture and in preclinical animal models [8, 9]. Glioblastoma multiforme (GBM) is the most common form of primary brain tumor and one of the most aggressive human cancers [10]. Current standard of care, involving surgery, irradiation and chemotherapy [11], remains palliative, with a median survival of 14 months. Consequently, novel treatments are an urgent unmet medical need. Glioma formation and growth have been associated with various molecular dysfunctions involving genes like c-Met, Notch-1/2 and cyclin-dependent kinase 6 (CDK6), which are known as target genes of miR-34a [12]. Overexpression of these oncogenes is recognized to play an important role in glioma cell survival, migration and proliferation [13]. This laid the basis for our research to employ miR-34a as an anticancer agent, which may lead to the inhibition of multiple survival pathways in glioma cells. However, miRNA replacement therapy is hindered by multiple physiological and cellular barriers. Due to their polyanionic nature, naked miRNAs display reduced uptake and poor intracellular trafficking, where sequestration in endosomes is one of the major obstacles to RNAi efficacy [2]. Moreover, when administered *in vivo,* miRNAs exhibit a poor pharmacokinetic profile due to their high susceptibility to serum nucleases, rapid renal clearance and nonspecific biodistribution [14]. To overcome these challenges, both viral vectors and nonviral delivery systems have been developed. Viral vectors are efficient delivery agents but may display toxicity and immunogenicity when introduced *in vivo* [15]. Most nonviral delivery systems, composed of synthetic materials, although demonstrated great promise as carriers for DNA [16], siRNA and miRNA showed remarkable limitations when evaluated *in vivo* [17]. Polymer therapeutics have attracted increasing attention over the last

4

few decades; a broad range of modified polymers is constantly being developed to improve the delivery of therapeutic agents to their target site [2, 18]. In order to serve as a drug delivery vehicle, a polymer needs to display some unique features which taken together will improve the pharmacokinetic and pharmacodynamic profile of the therapeutic agent. Polymer-based delivery systems can pursue these criteria by controlling their molecular composition, particle size, and surface properties to achieve specific biodistribution *in vivo* [19].

Nanogels (NGs) have emerged as a class of interesting polymeric materials for the delivery of small molecules and biomacromolecules [20-22]. NGs are nanosized hydrogel particles with three-dimensional networks composed of water-soluble/swellable polymers [21]. They have been recognized as promising drug delivery vehicles, owing to their high degree of porosity to incorporate a wide variety of bioactive molecules, desirable mechanical softness to positively affect cellular uptake and thereby biodistribution, large surface area for multivalent conjugation and high water content to ensure biocompatibility [23-26]. Recently, there has been a significant increase in the applicability of NGs for the delivery of therapeutic genes [27, 28]. Raemdonck *et al.* reported the preparation of cationic dextran-based NGs to efficiently silence a luciferase gene in hepatoma cells with negligible toxicity [29]. Moreover, delivery of siRNA to a variety of tissues *in vivo* has been successfully achieved by NGs [30]. Loading of a biological agent, e.g., miRNA, is usually achieved spontaneously through electrostatic interactions between the agent and the NGs matrix. As a result, the nano-structured gel collapses, forming stable nanoparticles [26]. This unique feature of NGs enables them to have relatively high loading capacity while keeping a small particle size.

Although the crosslinked NG network has shown promising potential for DNA/siRNA delivery, the suitable release profile in the specific locations is achieved by optimizing the structure of the NG network [23, 31]. Recently, the preparation of biodegradable disulfide crosslinked NGs, based on dendritic polyglycerol for the successful delivery of hydrophobic drugs such as doxorubicin, has been efficiently accomplished in our group using inverse nanoprecipitation [25]. These NGs can be efficiently internalized by tumor cells and thereafter, could be degraded/cleaved making use of intracellular reductive conditions. In order to exploit these NGs for delivery of oligonucleotides (DNA/siRNA/miRNA), cationic moieties were introduced into the predominant disulfide containing NGs for polyplex/complex formation. The resulting cationic NGs provide hydrophilicity, biodegradability, optimized size of the matrix, and biocompatibility for the efficient miRNA complexation, intracellular delivery, and gene silencing. The primary amine groups in the NGs had a relatively high pKa and were protonated at neutral pH, giving the nanogels positive charge to bind miRNA and facilitating cellular uptake via endocytosis [32]. The secondary amine groups in the NGs had a lower pKa and were further protonated at endosomal pH, providing the nanogels with endosomal escape capacities. Multiple amino groups were previously demonstrated to behave as endosomal buffering agents that facilitate the oligonucleotide's endosomal escape by a mechanism termed "the proton sponge effect" [33]. We therefore evaluated the effect of the addition of multiple amino groups to the nanogels on the efficiency of the transfection. The disulfide groups are stable in extracellular media but cleaved inside the cell cytoplasm due to presence of glutathione (GSH) [34], which is elevated in cancer cells as compared to normal cells [35]. After endosomal escape,

6

these reduction-sensitive degradable NGs can dissociate and release the miRNA in the cytoplasmic reductive environment.

Herein, we investigated six polymeric NGs, based on a polyglycerol-scaffold (referred as NG1, NG2, NG3, NG4, NG5, and NG6). We evaluated the capability of these NGs to encapsulate miR-34a and neutralize its negative charge in a dose-dependent manner. We have hypothesized that miR-34a replacement therapy, delivered by our NGs, may inhibit gliomas malignancy via downregulation of miR-34a target oncogenes. We hereby show a proof of concept for miR-34a delivery and anticancer activity in a human GBM mouse model. Human U-87 MG GBM cells transfected with NG-miR-34a nano-polyplexes showed significant downregulation of miR-34a known target genes. Treatment of SCID mice bearing human U-87 MG GBM with NG-miR-34a showed remarkable inhibition of tumor growth as opposed to treatment with NG-negative control miRNA and saline. This NG-miRNA platform may be the basis for a new therapeutic approach for GBM and hopefully pave the way in the future, for other types of cancer as well.

MATERIALS AND METHODS

Materials

Tissue culture reagents were purchased from Biological Industries Ltd. (Kibbutz Beit Haemek, Israel), unless otherwise indicated. General chemical reagents, including salts and solvents, were purchased from Sigma-Aldrich Israel (Rehovot, Israel), Aldrich (Germany) and Fluka (Germany). miR-34a mimic and negative control miRNA (NC-miR) were purchased from BioSpring GmbH (Germany) according to the following sequences:

7

miR-34a guide strand: 5Ph/UGGCAGUGUCUUAGCUGGUUGU, passenger strand: CAAUCAGCAAGUAUACUGCCCU; Negative control (NC) guide strand: 5Ph/TGGACTCTGAGAAAGGAGTATG, passenger strand: TACTCCTTATCAGACTCCATA.

Disulfide crosslinked NGs (NG6) were synthesized according to the previously reported technique [36]. Boc-glycine4-nitrophenyl ester, 4-dimethylaminopyridine (DMAP), trifluoroacetic acid (TFA), methanesulfonyl chloride (MsCl), ethylenediamine (EDA), diethylenetriamine (DTA), 4-bromobutyryl chloride, and triethylamine (TEA) were purchased from Aldrich (Germany). Dialysis tubes (molecular weight cut-off 2000) were obtained from Spectrum Laboratories, Inc. (Rancho Dominguez, CA, US).

Characterization

^{1}H NMR spectra were recorded on a Bruker ECX 400 operating at 400 MHz by using the residual deuterated solvent peaks as internal standard. Dynamic light scattering (DLS) measurements were carried out at 25°C using a Zetasizer Nano-ZS from Malvern Instruments equipped with a 633 nm He-Ne laser. Elemental analysis was performed by Elemental Analyzer VARIO EL.

Synthesis of NG1 and NG2

NGs (1 g, 13.5 mmol OH groups, 1 eq.) were suspended in 50 mL anhydrous DMF and the suspension was cooled to 0°C using an ice bath. A catalytic amount of DMAP was added, followed by the addition of Boc-glycine4-nitrophenyl ester (1.8 g or 3 g, for NG1 and NG2, respectively) to the reaction mixture, which was stirred overnight. After being concentrated into a small volume, the suspension was dialyzed in methanol for 3 days, and the Boc-protected

products respectively with 30% (Boc-protected NG1) and 50% (Boc-protected NG2) functionalities were obtained by drying under high vacuum. Regarding the deprotection of Boc-group, the excess methanol was evaporated to a volume of 5 mL and an equal amount of TFA was added with continuously stirring. After extensive dialysis in milli-Q-water, NG1 (functionality 30%, yield 48%) and NG2 (functionality 50%, yield 40.5%) were obtained by lyophilization. All aqueous solutions were freeze-dried with a Martin Christ Alpha 1-2 LD lyophilizer, for at least 12 hours.

^{1}H NMR (Boc-protected NG1, 400 MHz; CD_3OD): δ = 5.35-4.92 (0.3, functionalized secondary PG groups in NG), 4.45-4.05 (1.55, functionalized primary PG groups in NG), 4.01-3.36 (13.29, PG backbone), 1.78-1.15 (9.00, Me in Boc group).

^{1}H NMR (Boc-protected NG2, 400 MHz; CD_3OD): δ = 5.35-5.08 (0.40, functionalized secondary PG groups in NGs), 4.52-4.09 (1.37, functionalized primary PG groups in NGs), 4.07-3.41 (9.46, PG backbone), 1.59-1.12 (9.00, Me in Boc group).

^{1}H NMR (NG1, 400 MHz; D_2O): δ = 5.56-5.23 (functionalized secondary PG groups in NGs), 4.65-4.29 (functionalized primary PG groups in NGs), 4.25-3.41 (PG backbone).

^{1}H NMR (NG2, 400 MHz; D_2O): δ = 5.51-5.26 (functionalized secondary PG groups in NGs), 4.67-4.22 (functionalized primary PG groups in NGs), 4.18-3.36 (PG backbone).

Synthesis of NG3 and NG4

Mesylated NG (NG-OMs) was synthesized according to the following procedure. NG (1 g, 13.5 mmol OH groups, 1 eq.) was suspended in 50 mL anhydrous pyridine in a 250 mL round bottom flask having a dropping funnel. The suspension was cooled at 0°C using ice bath and the solution of MsCl (1.5 eq. 2.32 g) in 10 mL anhydrous pyridine was added dropwise with

continuous stirring below 5°C. The mixture was then allowed to stir overnight in the thawing ice bath and then crushed ice was added in the reaction mixture. A dark brown solid precipitated which was washed with distilled water after decantation of the liquid phase. The brown precipitate was dissolved and dialyzed in acetone to obtain a brown semi-solid NG-OMs after drying under high vacuum. NG-OMs (1 g, 11.36 mmol, 1 eq.) was then suspended in 20 mL DMF in a 50 mL three-neck flask. EDA (7.6 mL, 10 eq.) or DTA (12.2 mL, 10 eq.) were dropwise added via a syringe under the protection of argon and the reaction mixture was left heating at 40°C. After 2 days, both the reaction mixtures were concentrated to smaller volume, and subsequently dialyzed in methanol. Afterwards, the solutions were further concentrated to a volume of 5 mL by evaporating the excess methanol and 5 mL trifluoroacetic acid (TFA) was then added to these two solutions, under extensive stirring. NG3 (functionality 83%, yield 71%) and NG4 (functionality 80%, yield 67%) were obtained after dialyzing in Milli-Q-water, followed by lyophilization.

^{1}H NMR (NG-OMs, 400 MHz; acetone-D_6): δ =5.15-4.79 (0.56, functionalized secondary PG groups in NGs), 4.68-4.22 (0.89, functionalized primary PG groups in NG), 4.38-3.4 (3.58, NG backbone), 3.17 (3.00, Me in Ms group).

^{1}H NMR (NG3, 400 MHz; CD_3OD): δ = 3.12-2.41 (13.22, -$NH_2CH_2CH_2NH_2$), 4.37-3.42 (30.28, PG backbone), 3.19 (3.00, Me in EDA).

^{1}H NMR (NG4, 400 MHz; CD_3OD): δ = 3.11-2.7 (11.55, -$NHCH_2CH_2NHCH_2CH_2NH_2$), 4.38-3.41 (26.78, PG backbone), 3.17 (3.00, Me in ETA).

Synthesis of NG5

10

NG5 was synthesized by the following two step reactions. Firstly, NG (1 g, 13.5 mmol OH groups, 1 eq.) was suspended in 50 mL anhydrous pyridine and the suspension was cooled to 0 °C by ice bath. 4-bromobutyryl chloride (1.5 eq. 1.17 mL) was added dropwise into the reaction mixture followed by continuous stirring for 24 hours. Then, the mixture was dialyzed in methanol and the NG-Br was obtained. Secondly, 800 mg of NG-Br was suspended in 30 mL acetonitrile in the presence of 1 g of sodium iodide, and then an excess amount of TEA was added dropwise into the reaction system. The reaction was left stirring at 70°C for 3 days. Afterwards, the reaction mixture was filtered and the filtrate was extensively dialyzed against milli-Q-water, followed by lyophilization to obtain NG5 (functionality 32%, yield 42%).

^{1}H NMR (NG5, 400 MHz; D_2O): δ = 5.30-4.95 (0.80, functionalized secondary PG groups in NGs), 4.46-3.88 (2.86, functionalized primary PG groups in NGs), 3.85-3.40 (11.05, NG backbone), 3.363-3.065 (6.73, $(CH_3CH_2)_3NCH_2CH_2CH_2-)$, 2.54 (2.04, $-NCH_2CH_2CH_2-)$, 1.99 (2.00, -$NCH_2CH_2CH_2-)$, 1.24 (7.52, $(CH_3CH_2)_3N-)$.

Cell culture

U-87 MG cells were obtained from the American Type Culture Collection (ATCC; Manassas, USA). Cells were maintained in Dulbecco's modified Eagles's medium (DMEM) supplemented with 10% fetal bovine serum (FBS), 1% penicillin/streptomycin/nystatin, and 1% L-glutamine (Biological Industries, Israel). Cells were incubated at 37°C with 5% CO_2.

NG Polyplex formation

Six newly synthesized NG derivatives (referred as NG1, NG2, NG3, NG4, NG5, NG6) were evaluated for their ability to form a polyplex with miRNA. Each polyplex sample was prepared by mixing miRNA (miR-34a or the non-targeting miR (NC-miR)) and the NG specified at an indicated N/P ratio (ratio of nitrogen groups (N) on NGs to phosphate (P) of miRNA) in water solution for 20 minutes at room temperature (RT). For the evaluation of the formed complexes, as examined by electrophoresis mobility shift assay, the six NGs were allowed to form complexes with miR-34a at a final concentration of 0.083 µmol/L miR/water. We initially screened for a wide range of N/P ratios for each NG compound in order to find the minimal ratio which best stabilizes the miR. The ratios examined were: NG1 (N/P 0, 25, 50, 100), NG2 (0, 2.5, 5, 10, 25, 50), NG3 (0, 2, 5, 10), NG4 (0, 2, 5, 10, 50), NG5 (0, 2, 5, 10, 25), *NG6 (0, 100%, 20%, 5%, 2%). *N/P ratio of NG6 could not be determined due to the absence of amines on the molecule. Therefore, values of NG6 are presented as percentage from a concentration of 10 mg/mL.

Physico-chemical characterization of obtained polyplexes

Evaluation of polyplex formation by electrophoretic mobility shift assay (EMSA)

Formation of complexes between miR-34a and the different NG derivatives was confirmed by electrophoresis mobility shift assay (EMSA). Different N/P ratios were evaluated in a dose-dependent manner. The formed polyplexes were loaded on a 2% agarose gel. Electrophoresis was performed (100 V for 30 minutes) and visualized by ethidium bromide staining. In each gel, free miRNA was loaded as a reference.

12

Polyanion competition assay

The relative stability of the polyplexes was evaluated by measuring miRNA release in the presence of a competing polyanion, heparin [37]. Polyplexes were incubated in the presence of increasing amounts of heparin (0, 0.1, 0.15, 0.2, 0.25, 0.3, 0.8 IU) per 20 μL final volume of water for 15 minutes, then loaded on a 2% agarose gel, evaluated by electrophoresis at 100 V for 30 minutes and visualized by ethidium bromide staining. In each gel, free miRNA was loaded as a reference.

Size distribution and surface charge measurement (zeta potential) of polyplexes

DLS and zeta-potential measurements were performed on miR/NG nanoparticles using Zetasizer Nano ZS analyzer with an integrated 4 mW He-Ne laser (λ=633 nm; Malvern Instruments Ltd.). Samples were prepared by dissolving 0.125 mg/mL NG in 4-(2-hydroxyethyl)-1-piperazineethanesulfonic acid (HEPES) buffer (10 mM) at pH 7.4 and RT. miRNA was incubated with the selected NGs at the indicated N/P ratios for 20 minutes. Particles size and surface charge analyses were conducted only on the NG derivatives that efficiently formed complexes with miR-34a. DLS analysis results are specified according to intensity distribution.

Scanning Electron Microscope (SEM) images of polyplexes

Scanning electron microscopy (SEM) micrographs of the polyplexes were acquired using a Quanta 200 FEG Environmental SEM , in high vacuum and accelerating voltage of 5.0 KV. Each NG solution of 0.3 mg/mL was mixed with miR-34a (N/P=5) and incubated at RT for 20 minutes. The polyplex solution was placed onto the surface of Silicon (Si) wafer, air-dried for 20 minutes and then covered with a 4 nm layer of Chromium (Cr). Analysis of polyplexes size was acquired with measureIT® software and determined by the average of 3 fields, 40 particles per field.

Evaluation of polyplexes' cellular uptake and intracellular trafficking by confocal microscopy

U-87 MG mCherry-labeled GBM cells were seeded on cover slides and grown overnight (1×10^5 cells/slide). Cy5-labeled miR-34a (50 pmol, 100 nM final concentration) (Integrated DNA Technologies) was allowed to form complexes with the indicated NGs [NG2/miR-34a (N/P=25) and NG3/miR-34a and NG4/miR-34a (both N/P=5) and then added to the cells. Cells were incubated with miRNA alone or with NG/miRNA polyplexes for 30 minutes, 2, 4, 8 and 24 hours. Following exposure to treatment, cells were washed three times with PBS, fixed with 4% paraformaldehyde (PFA) solution for 20 minutes at RT and washed again with PBS. Cover glasses were then mounted with VECTASHIELD® DAPI-containing medium (Vector Laboratories, USA). Confocal images were acquired with a Leica TCS SP8 confocal imaging system (Leica Microsystems, Wetzlar, Germany).

Evaluation of miRNA levels by real-time quantitative PCR (RT-qPCR)

Expression levels of miR-34a and its target genes were assessed by RT‑ qPCR following treatment with miR/NG polyplexes. U-87 MG GBM cells (3×10^5 cells /well) were seeded in 10 cm plates (37°C; 5% CO_2). Twenty-four hours later U-87 MG cells were transfected with 200 nM miR-34a or NC-miR complexed with the indicated NGs [NG3/miR-34a and NG4/miR-34a both N/P=5] or left untreated. Total RNA was extracted (EZ-RNA II, Biological Industries) from each sample and subjected to reverse transcription into cDNA (miSCript II RT, Qiagen). Samples were evaluated for the expression levels of miR-34a and its target genes using SYBR green real-time qPCR (StepOne plus, Life Technologies). miR-34a expression levels were evaluated by miSCript miRNA primer assays (Qiagen, USA) according to the manufacturer's protocol and were normalized to RNU6. Expression levels of miR-34a target genes were assessed using custom

made primers (Syntezza Bioscience, Israel) and SensiFAST^{TM} SYBR green (Bioline, United Kingdom) according to manufacturer's protocol, and were normalized to Actin. Target genes primers pairs were:

C-MET: F – CAGTGGTGGGAGCACAATAA, R – TGTAAAGTTCCTTCCTGCTTCA; CDK6: F – TCACGAACAGACAGAGAAACC, R – CTCCAGGCTCTGGAACTTTATC; Notch1: F – CCCACAAGGTGTCTTCCAG, R – AGGATCAGTGGCGTCGTG; Bcl-2: F – GGCCAGGGTCAGAGTTAAATAG, R – GGAGGTTCTCAGATGTTCTTCTC; Actin: F – CCAACCGCGAGAAGATGA, R - CCAGAGGCGTACAGGGATAG.

Evaluation of the anticancer activity of the polyplexes

Evaluation of U-87 MG cells viability following treatment with the polyplexes

U-87 MG GBM cells (8×10^3 cells/well) were seeded in 24 well plates (37 °C; 5% CO$_2$). Twenty-four hours later, cells were transfected with 50, 100, 200 nM miR-34a or NC-miR complexed with the indicated NGs [NG3/miR-34a and NG4/miR-34a both at N/P=5] or left untreated. NG/miR-34a or NG/NC-miR polyplexes. Following 120 hours incubation, the number of viable cells was counted by a Z1 Coulter Counter® (Beckman Coulter).

In vivo **studies**

All *in vivo* procedures were performed in accordance with the National Institutes of Health (NIH) animal care guidelines and approved by Tel Aviv University institutional animal care and use committee (IACUC). All animals were allowed free access to food and water during the experiments.

15

Evaluation of the anticancer efficacy of the polyplex using a U-87 MG GBM xenograft model

U-87 MG GBM cells were inoculated subcutaneously in the flank of SCID mice (6-8 weeks old, male, 20 to 25 g body weight) (Harlan Laboratories, Israel). Tumor volume was monitored and calculated as length x width^2 x 0.52. When the tumor reached a volume of ~70 mm^3, mice were randomly divided into the experimental groups (n = 5-6/group). Mice were injected intratumorally (30 μl per injection) with saline (control), miR-34a or NC-miR (4 mg/kg miR complexed with the specific NG at N/P=5) on days 0, 3, 7 and 10. Tumor volume, body weight, behavior and general health were monitored twice a week.

Statistical methods

For *in vitro* assays, data was expressed as mean ± standard deviation (s.d.) and statistical analysis was performed using a student's T-test. For *in vivo* assays, data was expressed as mean ± standard error of the mean (s.e.m.) and statistical analysis was performed using an ANOVA with repeated measures.

RESULTS

Synthesis of NGs

Disulfide crosslinked NGs, which are degradable under intracellular reductive conditions, were prepared by a published inverse nanoprecipitation technique [36, 38]. Five cationic NGs, NG1-5, were synthesized by introducing amino containing functionalities as shown in Scheme S1, Table S1 and summarized in Figure 1. The functionalization percentages were calculated by the integral ratio between the amino-bearing moieties and dendritic polyglycerol in the ^{1}H NMR spectra. Zeta potential and hydrodynamic diameter of the polyplexes were measured under pH

16

7.4 at 37 °C (Table S2). We used a 21-mer double-stranded DNA for measuring the size and charge of the colloidal solutions of NGs-polyplex in the present study. This 21-bp DNA molecule has been used in previous studies as an appropriate general model for physicochemical characterization of polyamine polyplexes [39-43]. At all the N/P ratios evaluated (Table S2), the polyplexes had an approximate size of 200 nm with positive charge and the zeta potential increased in parallel to the N/P ratio. Notably, no large aggregates were formed for all the evaluated N/P ratios, since the electrostatic repulsion induced by the high zeta potential could keep the colloidal stability.
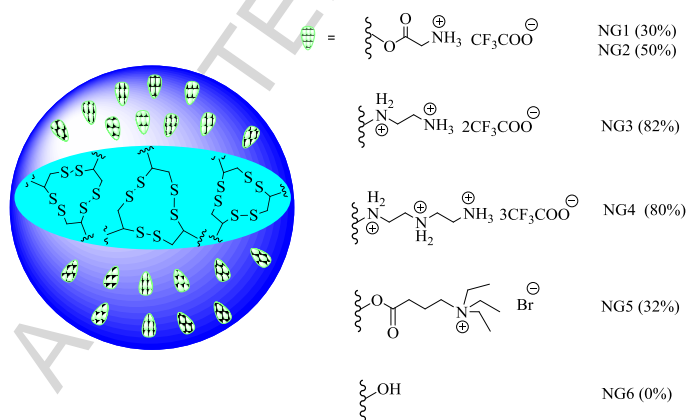

Figure 1. Schematic representation of the degradable nanogels bearing different amine-bearing moieties.

Formation of NG/miR-34a polyplexes

The capability of six NGs (referred to as NG1-NG6) to form self-assembled complexes with miR-34a was examined by an electrophoresis mobility shift assay (Figure 2). Different amounts of NGs were incubated with a fixed amount of miR-34a and the ability to assemble a complex was

monitored via the delayed mobility of the miRNA in an agarose gel. As shown, only NG2, NG3 and NG4, which contained sufficient amine end groups, were able to bind miRNA and neutralize its negative charge in a dose-dependent manner (Figure 2B, 2C, 2D). NG2 formed a polyplex with miRNA in a relatively high N/P ratio, compared to NG3 and NG4, probably due to its lower amine content. No mobility shift of miRNA was observed following incubation with the carrier NG1 and NG5, probably due to their low amine contents and the steric hindrance that resulted from the triethyl amine linker of NG5 (Figure 2A and E).NG6 did not form a complex with miR-34a, presumably due the lack of free amine residues which are essential for the binding of the miRNA (Figure 2F). Based on the electrophoretic mobility shift assay results, we continued our research with NG2, NG3, and NG4 nanocarriers.
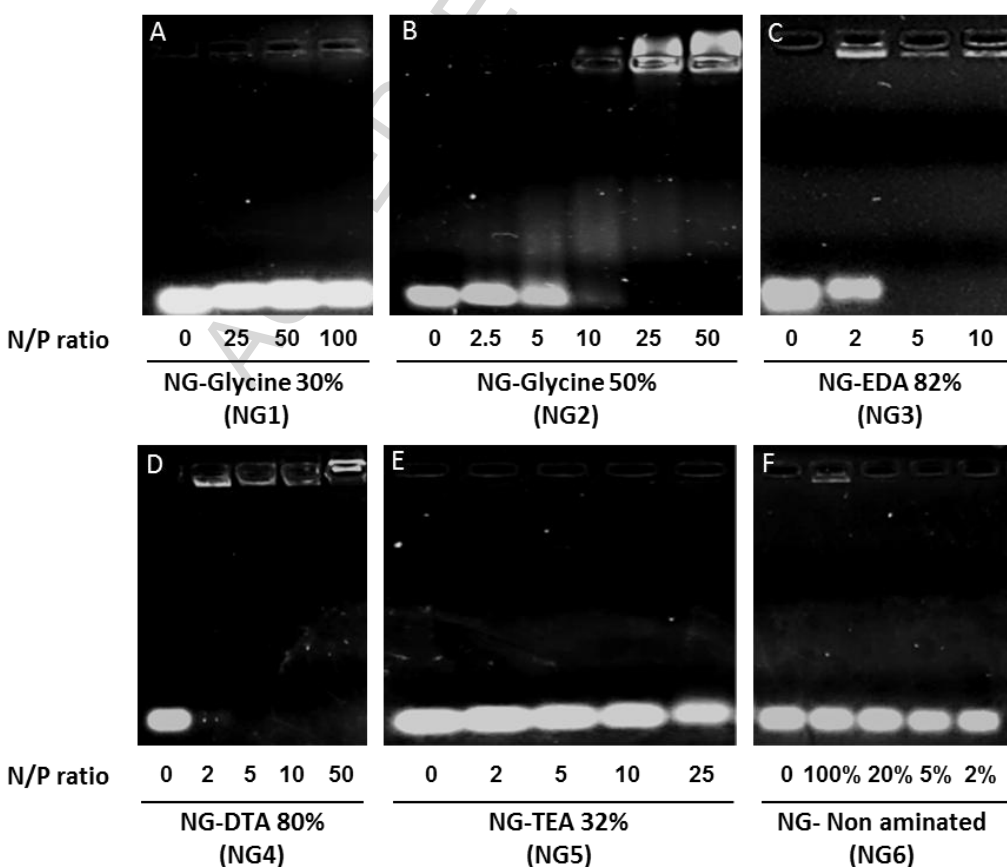

N/P ratio				
0	25	50	100	

NG-Glycine 30% (NG1)

| 0 | 2.5 | 5 | 10 | 25 | 50 |

NG-Glycine 50% (NG2)

| 0 | 2 | 5 | 10 |

NG-EDA 82% (NG3)

| N/P ratio | | | | |
| 0 | 2 | 5 | 10 | 50 |

NG-DTA 80% (NG4)

| 0 | 2 | 5 | 10 | 25 |

NG-TEA 32% (NG5)

| 0 | 100% | 20% | 5% | 2% |

NG- Non aminated (NG6)

18

Figure 2. Electrophoresis Mobility Shift Assay of six evaluated NGs complexed with miR-34a. Migration of NGs/miR34a polyplexes at different N/P ratios. **A.** NG1/miR-34a. **B.** NG2/miR-34a. **C.** NG3/miR-34a. **D.** NG4/miR-34a. **E.** NG5/miR-34a. **F.** NG6/miR-34a. * N/P ratio of NG6 could not be determined due to the absence of amines on the molecule. Therefore, values of NG6 are presented as percentage from a concentration of 10 mg/mL.

Physico-chemical characterization of NG/miR-34a polyplexes

Size and surface charge of the three selected NGs were determined by DLS and zeta potential measurements (Table 1). As can be seen, the polyplexes NG2/miR-34a, NG3/miR-34a and NG4/miR-34a formed nano-sized particles (NG2 polyplex: 160 nm, NG3 polyplex- 168 nm and NG4 polyplex- 141 nm). Based on these findings, we speculated that these NGs formed a stable supramolecular structure with miRNA such as those formed with DNA (Table S2). Similarly to recent studies that demonstrated increase in zeta potential in correlation to the amine content of polyplexes [44]**,** the transition from ester bond (NG2) to secondary amine (NG3), and the addition of another secondary amine (NG4), resulted in an increased zeta potential. It has been considered that when the zeta potential (absolute value) is above 30 mV, the nanoparticles are physically stable due to the presence of electrostatic repulsion [45]. The zeta potential of polyplexes NG2 was 27.9 ± 7.36 mV, which is much lower than that of polyplexes NG3 (46.2 ± 7.3 mV) and NG4 (50.5 ± 7.06 mV). Therefore, it could be presumed that more aggregation occurred in polyplexes NG2, resulting in the considerable polydispersity index of NG2 compared to NG3 and NG4.

Interestingly, we observed an inverse correlation between the size of the nanoparticles and the length of the aminated linkers on NG3 and NG4 (see NGs chemical structure in Table S1). Based on that, we postulated that the amine modified linker on NG3, composed of ethylenediamine,

19

led to the formation of relatively larger particles in size, compared to the ones formed by NG4 (contains diethylenetriamine linker), as the longer chain resulted in more closely packed complexes. Zeta potential measurements revealed that all polyplexes exhibited positive surface charge.

Table 1. Hydrodynamic diameter and zeta potential measurements of NG2/miR-34a NG3/miR-34a and NG4/miR-34a polyplexes.

	N/P ratio	DLS		Zeta potential [mV]
		Hydrodynamic diameter [nm]	PDI	
NG2	25:1	160± 45	0.371	27.9 ± 7.36
NG3	5:1	168 ± 76	0.178	46.2 ± 7.3
NG4	5:1	141 ± 61	0.168	50.5 ± 7.06

SEM micrographs of NG3/miR-34a and NG4/miR-34a polyplexes (Figures 3A and 3B, respectively) revealed a spherical shape of the nanoparticles. Size obtained from the SEM data was similar to the size trend observed from the DLS measurements, as NG3 formed a larger complex than NG4 (181 ± 33 *versus* 137 ± 39 nm in diameter, respectively). Size measurements are expressed as mean ± SD.
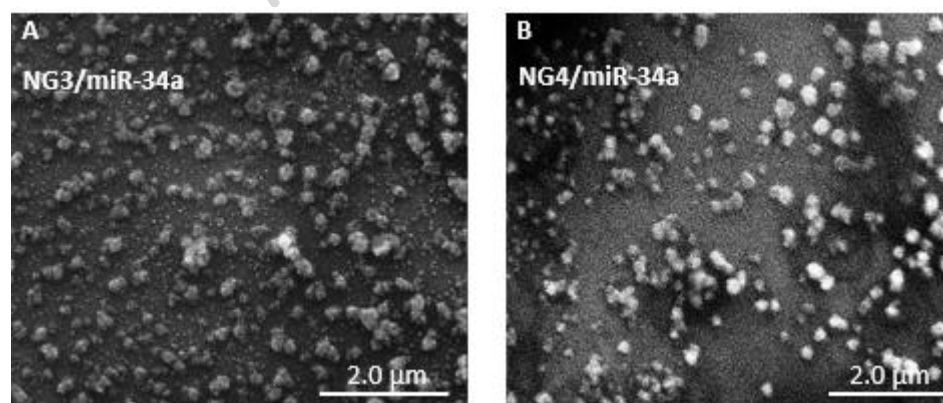

Figure 3. SEM micrograph of NG/miR-34a polyplex. **A**. NG3/miR-34a polyplexes. **B**. NG4/miR-34a polyplexes.

NGs enable internalization of miR-34a into mCherry-labeled U-87 MG GBM cells

In order to investigate the uptake and intracellular localization of the polyplexes, we used Cy5-labeled miR-34a. mCherry-labeled U-87 MG cells were incubated with the indicated polyplexes for 2, 8 and 24 hours. Minor internalization of NG2/miR-34 was detected within the cytoplasm of the cells, mostly 24 hours following treatment. In contrast, remarkable internalization of miR-34a was observed following complexation with NG3 and NG4 two hours following treatment. miR-34a internalization increased within 8 hours with maximum accumulation achieved 24 hours post-incubation (Figure 4). Intracellular localization of naked miRNA was hardly observed. Based on these findings demonstrating poor internalization of NG2/miR polyplexes, we did not continue further research with this carrier.
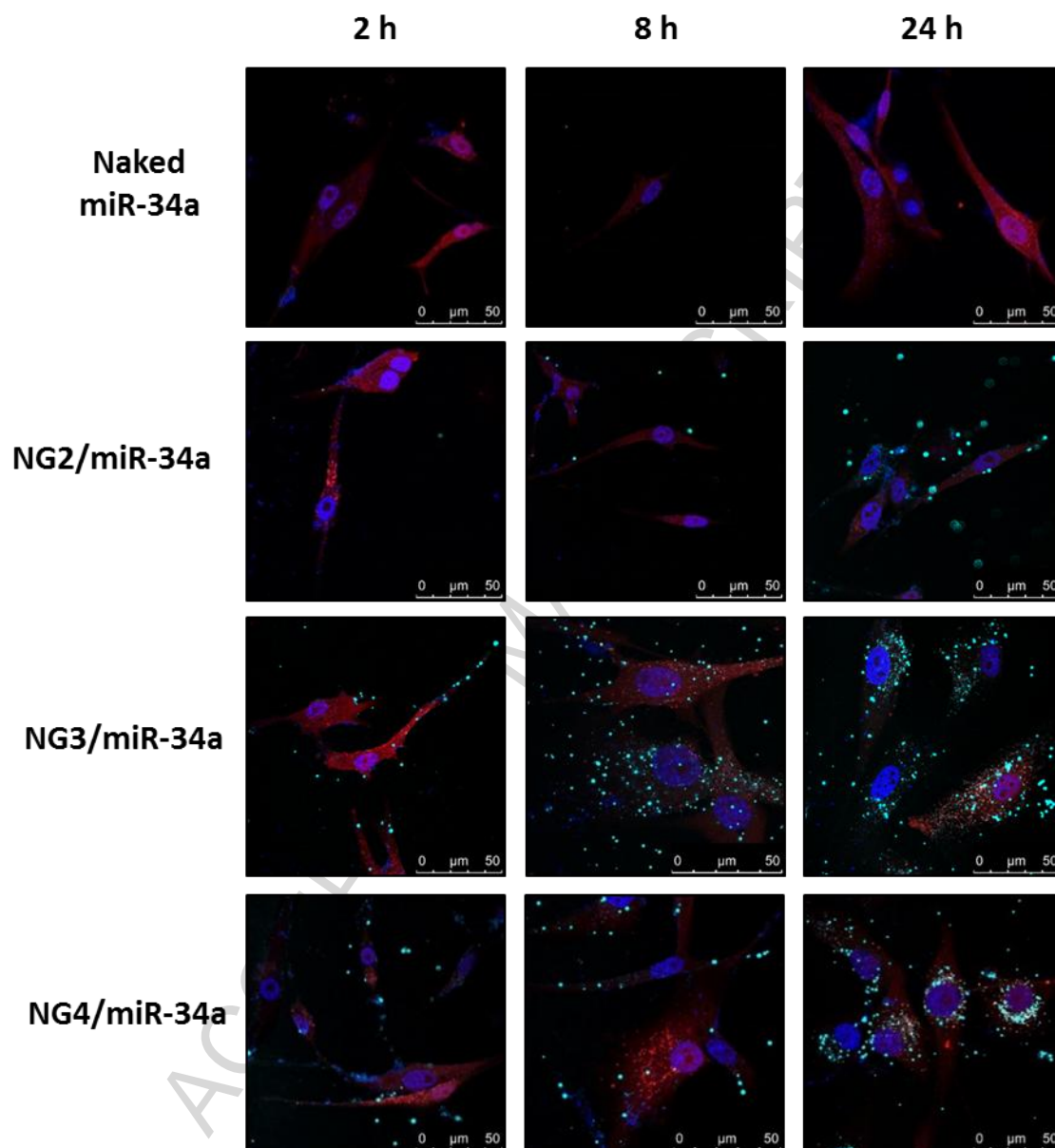
Figure 4. Intracellular uptake of NG/miR-34a in mCherry-labeled U-87 MG GBM cells. Confocal microscopy analysis of U-87 MG GBM cells after treatment with NG2/miR-34a (N/P=25) and NG3/miR-34a and NG4/miR-34a (both N/P=5). Confocal images indicate that NG/miR-34a polyplexes internalized in a time-dependent manner. Cy5-labeled miR-34a in complexation with NG3 and NG4, but not NG2, is localized at the cytoplasm of cells. Images were taken with a Leica SP8 confocal microscope. Scale bars represent 50 μm.

Delivery of miR-34a by NGs to U-87 MG GBM cells leads to upregulation of miR-34a and downregulation of its target genes

The tumor suppressive properties of miR-34a are attributed to downregulation of multiple oncogenes including c-MET [46], CDK6 [47], Notch1 [48] and Bcl-2 [49]). Overexpression of these oncogenes was reported to be associated with increased tumorigenicity of brain tumors including gliomas, and to correlate with poor prognosis [12, 50]. This suggests that forced expression of miR-34a may lead to downregulation of its target oncogenes, resulting in a potent anticancer effect on GBM.

We evaluated the expression levels of miR-34a following treatment of U-87 MG cells with NG/miR-34a polyplexes by qRT-PCR analysis. NG3/miR-34a and NG4/miR-34a polyplexes showed relatively similar transfection efficiency, leading to high expression levels of miR-34a, whereas NC-miR and untreated cells exhibited only low basal levels of miR-34a (Figure 5A). Treatment with NG3/miR-34a further induced downregulation of the miR-34a target genes C-MET, CDK6, Bcl-2 and Notch-1 (Figure 5B-5E). Interestingly, transfection with NG4/miR-34a did not result in a similar downregulation of these target genes (Figure 5B-5E), despite the notable transfection efficacy of the NG4 carrier (Figure 5A).
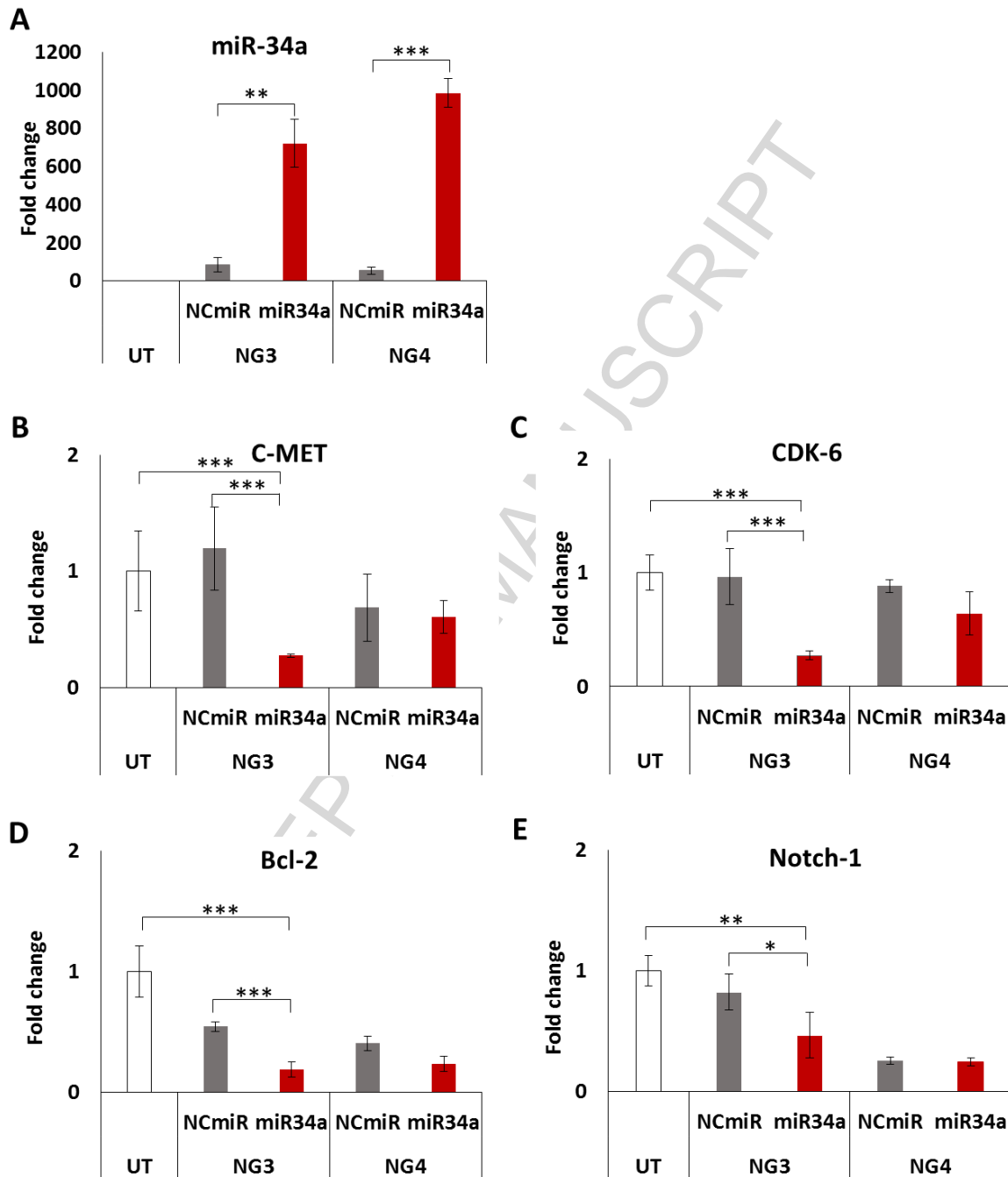
Figure 5. Quantitative RT-PCR analysis of miR-34a levels and its target genes in U-87 MG cells following treatment with NG/miR polyplexes. Transfection of miR-34a (200 nM) complexed with NG3 and NG4 nanocarriers down regulates miR-34a target genes. **A.** miR-34a expression levels. **B-E.** miR-34a target genes expression levels. Expression levels of C-MET, CDK6, Bcl-2 and Notch1 were normalized to Actin gene expression. *p value ‹ 0.05, **p value ‹ 0.03, ***p value ‹ 0.01.

NG/miR-34a inhibits proliferation of U-87 GBM cells

In order to establish a proof-of-concept for NG/miR-34a anticancer effect, we next treated U-87

MG cells with NG3/miR-34a and NG4/miR-34a polyplexes and evaluated the effect on cells

viability *in vitro*. U-87 MG cells treated with NG/miR-34a polyplexes displayed a decrease in cell

viability in a dose-dependent manner (Figure 6). In agreement with the qRT-PCR results,

NG3/miR-34a induces a more potent anti-proliferative effect than NG4/miR-34a. While the

NG3/miR-34a exhibits an IC_{50} of 100 nM, the IC_{50} of NG4/miR-34a is higher than 200 nM (miR-
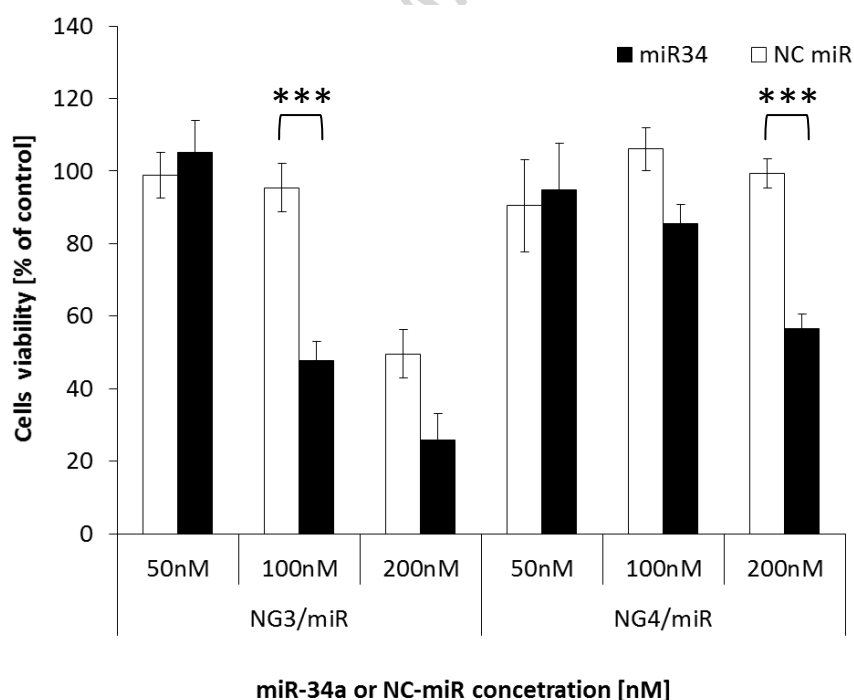
34a equivalent dose).

Figure 6. NG/miR-34a inhibits U-87 MG cells viability. The cytotoxic effect of miR-34a treatment
was measured by direct cell counting 120 hours following transfection of cells with NG3/miR-
34a and NG4/miR-34a compared to NG3/NC-miR, NG4/NC-miR or untreated control. Each value
represents the mean ± SD from triplicate determinations. ***p value ‹ 0.01.

NG/miR-34a polyplexes differ in their ability to release miRNA

In order to compare the stability of NG3/miR-34a and NG4/miR-34a polyplexes, we incubated the polyplexes in the presence of heparin as a competing polyanion to miRNA. As shown in Figure 7, the amount of heparin required to release miR-34a from NG4 was about 3-times higher compared to NG3 complex. Based on NG3 and NG4 chemical structure (Figure 1, Table S1), the size of the polyplexes (Table 1, S2) and the difference in the stability of the two (Figure 7), we hypothesized that miR-34a was strongly condensed when complexed with NG4 carrier as opposed to the polyplex formed with NG3 carrier.
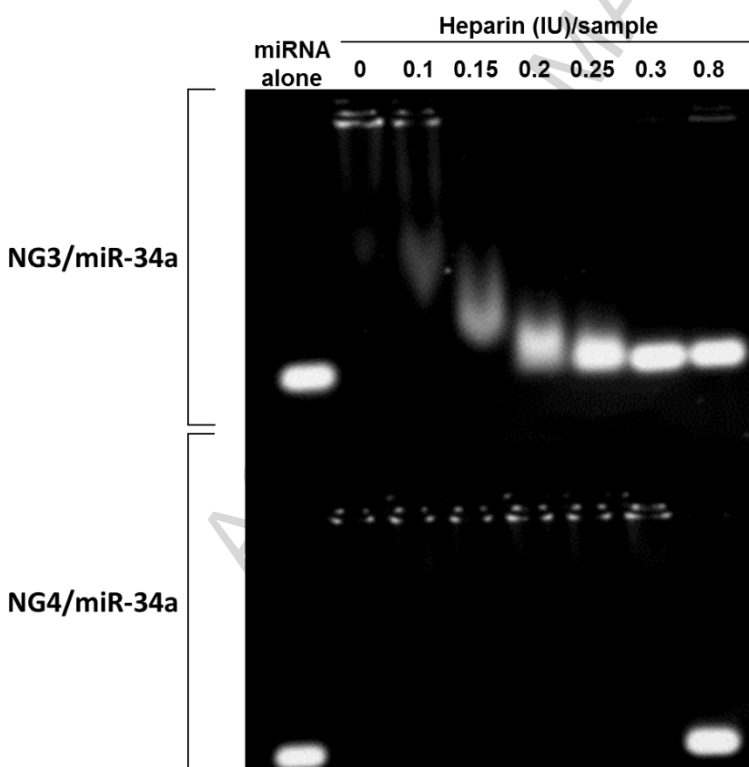

Figure 7. Polyanion competition assay. Relative stability of NG3/miR-34a and NG4/miR-34a polyplexes was determined by gel electrophoresis. The release of miR-34a from the carriers was evaluated in the presence of rising amounts of a competing polyanion heparin. Following the formation of the polyplexes, they were incubated in the presence of increasing concentrations of heparin (IU=international units).

NG3/miR-34a polyplexes inhibit tumor growth in a xenograft mouse model of GBM

We next studied the potential anti-tumor efficacy of NG/miR-34a polyplexes using a xenograft model of GBM, established by injection of U-87 MG cells to the flank of SCID mice. Once tumors reached the size of ~70 mm^3, mice were randomized into treatment groups and comparative efficacy studies began. Mice were injected intratumorally with NG3 and NG4 polyplexes (complexed with miR-34a or NC-miR) or with saline and tumor volume was measured twice a week by caliper. Dose (4 mg miRNA /kg mouse) was determined following a preliminary maximal tolerated dose (MTD) study (data not shown). NG3/miR-34a showed remarkable antitumor activity (Figure 8) in contrast to NG4/miR-34a. Local administration of NG3/miR-34a significantly inhibited tumor growth, as opposed to NG3/NC-miR and the control group treated with saline. The average tumor volume of the NG3/miR-34a treated group was substantially reduced (379±175 mm^3) *versus* the NG3/NC-miR (883±580 mm^3) or the saline-treated group (1197±359 mm^3) on day 20. NG4-based nanoparticles exhibited non-specific toxicity towards tumor cells, causing tumor growth inhibition when complexed with either miR-34a or NC-miR. Results clearly indicated that NG3/miR-34a polyplexes are substantially more specific and effective as anticancer therapy for GBM xenografts than NG4/miR-34a. These findings are in agreement with the *in vitro* observations, which demonstrated the clear advantage of NG3/miR-34a polyplex downregulating miR-34a target genes and inhibiting cell viability in comparison with NG4/miR-34a polyplex.
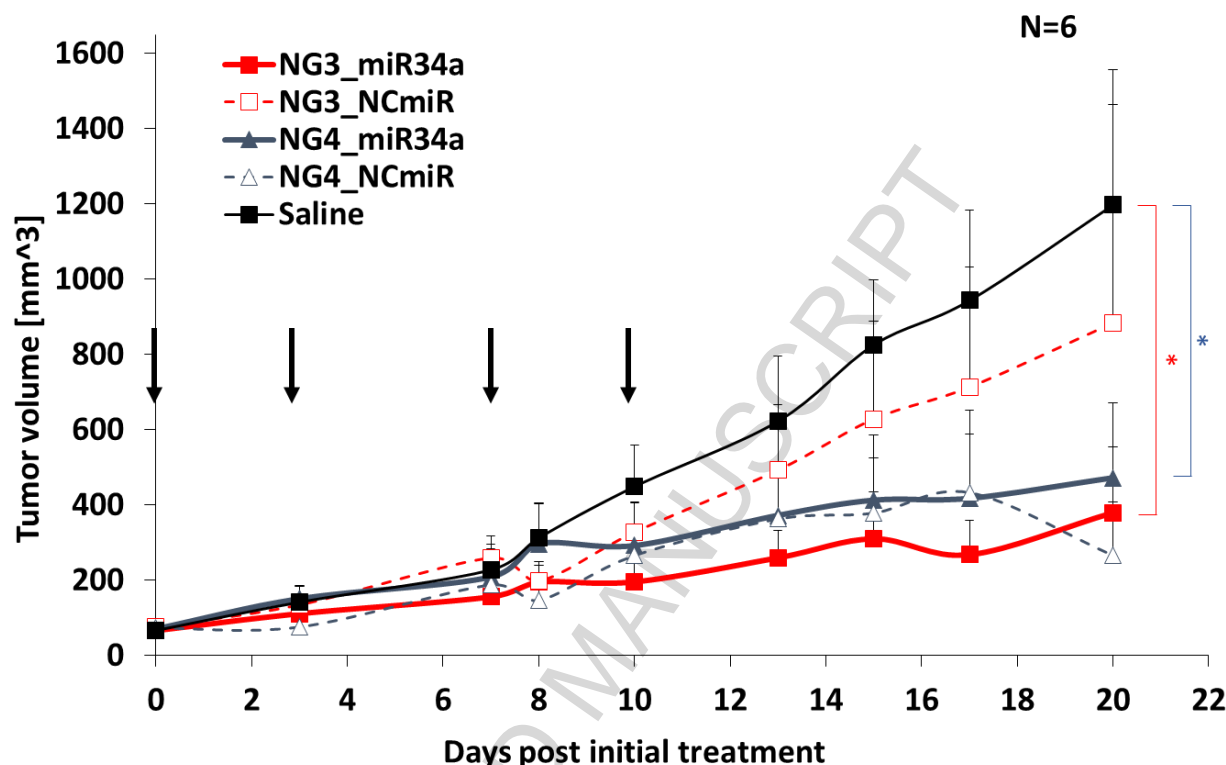
Figure 8. **NG/miR-34a polyplexes exhibit a substantial anti-tumor effect in U-87 MG xenograft model of GBM.** Mice (N=6/group) were injected intratumorally with miR-34a or NC-miR (4 mg/kg) complexed with NG3 or NG4, or saline. Mice were administered four consecutive treatments (on days 0, 3, 7 and 10, marked by black arrows in the graph). Data presented as mean ± s.e.m. *p value<0.01. ANOVA repeated measures statistical analysis displayed time by group interaction for the control treated saline group in comparison with NG3/miR-34a, NG4/miR34a and NG4/NC-miR groups.

DISCUSSION AND CONCLUSIONS

miRNA therapeutic potential highlights the need to design systems that will deliver miRNA to the target cells at the diseased tissue at clinically-relevant levels. A variety of nano-sized delivery systems has been developed to improve miRNA delivery and uptake both *in vitro* and *in vivo*, including liposomes [51], peptides, antibodies [52], small molecule ligands [53] and polymeric nanoparticles [54]. In spite of all current attempts, there is no FDA- or EMA-approved

RNAi-complex yet. Investigating the relationship between the carrier and the cargo, and their physico-chemical properties, structure, and biological function is fundamental in designing an adequate miRNA delivery system. miRNA has a negatively-charged phosphodiester backbone which allows it to interact electrostatically and be condensed when complexed with a cationic agent into a small nanoparticle [19]. The formed polyplex ensures that the miRNA is encapsulated and protected against enzymatic degradation and facilitates its cellular uptake and intracellular trafficking [55]. By virtue of their size and surface properties, nanoparticles can accumulate in the tumor site due to the enhanced permeability and retention (EPR) effect that allows extravasation-dependent accumulation across leaky vasculature [56].

The continuous need for functional polymeric systems which possess characteristics of a well-defined, monodispersed, stable nanostructures at the molecular level leads to the development of new methodologies and biomaterials in this field [57]. Amongst them are the NGs that came into view as polymeric scaffolds that fill the size gap between dendrimers/polymers, with diameters ranging from 10-20 nm, and the macroscopic hydrogels [20]. NGs are macromolecular architectures made of polymeric units cross-linked to each other in a supramolecular framework. These polymeric materials emerged due to their controllable size, shape, functionality, good mechanical properties, and the presence of a big void for the encapsulation of therapeutic cargo. The nanoscale mainly provides a large surface area for bioconjugation, long circulation time in the blood, and tunable size from nanometers to micrometers with the possibility of being actively- or passively-targeted to the desired site of action, e.g., tumor sites [22, 58].

In the present work, a novel approach for miR-34a delivery through the complexation of miR-34a with polyglycerol-based NGs has been established. A facile surfactant-free method, so-called inverse nanoprecipitation was used to synthesize redox-sensitive NGs, which are degradable under intracellular reductive conditions. Different amine-bearing moieties were attached to the polyglycerol units included within the NGs structure. Using the variable amine modified linkers on the NGs (refer to Figure 1 and Table S1 for NGs chemical structure) as tools to control the interactions between the NGs and the miRNA, we synthesized and characterized six potential nanocarriers for miR-34a delivery. We selected the nanocarriers according to their ability to bind miRNA in a stable manner, demonstrate enhanced cellular uptake, high transfection efficacy and downregulation of miR-34a target genes leading to inhibition of proliferation and migration of GBM cells. Nanocarriers NG3 and NG4 demonstrated high capability to complex miR-34a and neutralize its negative charge in a dose-dependent manner (Figure 2). In accordance with previous studies, cationic surface charge of nanoparticles plays a crucial role in the internalization capability of nanoparticles [59-61], thus explaining the lower uptake of the less positively charged NG2 compared with NG3 and NG4 polyplexes. in addition, the high polydispersity of NG2 polyplex indicates the formation of aggregates, that interrupt characterization of cellular uptake [57]. In addition, both NG3 and NG4 carriers were successful in delivering miR-34a to U-87 MG cells, as they were able to rapidly internalize into cells (Figure 4) and to significantly increase miR-34a levels following transfection (Figure 5). However, NG3/miR-34a polyplexes were superior to NG4/miR-34a polyplexes in their ability to knockdown miR-34a target oncogenes (Figure 5), to inhibit the proliferation of U-87 MG cells (Figure 6) and to inhibit U-87 MG tumor growth in mice (Figure 8). To explain these findings, we

30

rationalized that those differences may result from the distinct intracellular fate of the two polyplexes following internalization, which is, among other parameters, governed by the interaction strength between the NGs and the miRNA in the polyplex. We next evaluated the stability of NG3/miR-34a and NG4/miR-34a polyplexes by a polyanion competition assay (Figure 7). Results showed a remarkable difference between the capabilities of the two nanocarriers to release the miRNA, with an increased stability of NG4/miR-34a complex. The high stability of NG4/miR-34a polyplex can explain the discrepancy between the high level of cellular uptake of NG4 carrier and the nonspecific anticancer activity of the polyplex *in vitro* and *in vivo*. We hypothesized that miRNA is not successfully released from the NG4 carrier, leading to its reduced activity *in vitro*. Taken together, non-specific potent activity of the NG4/NC miR complex *in vivo* is evident by its increased toxicity not related to miR-34a oncogenic pathways compared with the not-active NG3/NC miR polyplex.

In contrast, NG3/miRNA polyplex is less stable, but apparently, it is stable enough time to allow efficient delivery of miR-34a to the cell cytoplasm following polyplex decomplexation. Therefore, NG3/miR-34a carrier demonstrated potent and specific anticancer effect both *in vitro* and *in vivo*.

In conclusion, we have demonstrated a concept of biodegradable NGs designed to deliver miR-34a to target GBM cells. NG3/miR-34a polyplex was able to restore the tumor suppressor role of miR-34a in U-87 MG GBM xenograft leading to remarkable inhibition of tumor growth. The comprehensive comparison between NG3/miR34a and NG4/miR34a polyplexes *in vitro* and *in vivo* provides new insights to some of the key features such as the fine

31

balance between stability and activity that should be taken into account when designing an

optimal delivery system for oligonucleotide-based therapeutics to tumor cells.

REFERENCES

[1] Jansson MD, Lund AH. MicroRNA and cancer. Molecular oncology. 2012;6:590-610.
[2] Tiram G, Scomparin A, Ofek P, Satchi-Fainaro R. Interfering cancer with polymeric siRNA nanomedicines. J Biomed Nanotechnol. 2014;10:50-66.
[3] Bader AG, Brown D, Winkler M. The promise of microRNA replacement therapy. Cancer Res. 2010;70:7027-30.
[4] Fujiwara T, Yada T. miRNA-target prediction based on transcriptional regulation. BMC Genomics. 2013;14 Suppl 2:S3.
[5] Bader AG. miR-34 - a microRNA replacement therapy is headed to the clinic. Front Genet. 2012;3:120.
[6] Calin GA, Dumitru CD, Shimizu M, Bichi R, Zupo S, Noch E, et al. Frequent deletions and down-regulation of micro- RNA genes miR15 and miR16 at 13q14 in chronic lymphocytic leukemia. Proc Natl Acad Sci U S A. 2002;99:15524-9.
[7] Croce CM. Causes and consequences of microRNA dysregulation in cancer. Nat Rev Genet. 2009;10:704-14.
[8] Gaur A, Jewell DA, Liang Y, Ridzon D, Moore JH, Chen C, et al. Characterization of microRNA expression levels and their biological correlates in human cancer cell lines. Cancer Res. 2007;67:2456-68.
[9] Liu C, Kelnar K, Liu B, Chen X, Calhoun-Davis T, Li H, et al. The microRNA miR-34a inhibits prostate cancer stem cells and metastasis by directly repressing CD44. Nat Med. 2011;17:211-5.
[10] Wen PY, Kesari S. Malignant gliomas in adults. N Engl J Med. 2008;359:492-507.
[11] Stupp R, Mason WP, van den Bent MJ, Weller M, Fisher B, Taphoorn MJ, et al. Radiotherapy plus concomitant and adjuvant temozolomide for glioblastoma. N Engl J Med. 2005;352:987-96.
[12] Purow BW, Haque RM, Noel MW, Su Q, Burdick MJ, Lee J, et al. Expression of Notch-1 and its ligands, Delta-like-1 and Jagged-1, is critical for glioma cell survival and proliferation. Cancer Res. 2005;65:2353-63.

[13] Li WB, Ma MW, Dong LJ, Wang F, Chen LX, Li XR. MicroRNA-34a targets notch1 and inhibits cell proliferation in glioblastoma multiforme. Cancer Biol Ther. 2011;12:477-83.

[14] Behlke MA. Progress towards in vivo use of siRNAs. Mol Ther. 2006;13:644-70.

[15] Thomas CE, Ehrhardt A, Kay MA. Progress and problems with the use of viral vectors for gene therapy. Nat Rev Genet. 2003;4:346-58.

[16] Whitehead KA, Langer R, Anderson DG. Knocking down barriers: advances in siRNA delivery. Nat Rev Drug Discov. 2009;8:129-38.

[17] Khatri N, Rathi M, Baradia D, Trehan S, Misra A. In vivo delivery aspects of miRNA, shRNA and siRNA. Crit Rev Ther Drug Carrier Syst. 2012;29:487-527.

[18] Duncan R, Ringsdorf H, Satchi-Fainaro R. Polymer therapeutics--polymers as drugs, drug and protein conjugates and gene delivery systems: past, present and future opportunities. J Drug Target. 2006;14:337-41.

[19] Howard KA, Kjems J. Polycation-based nanoparticle delivery for improved RNA interference therapeutics. Expert Opin Biol Ther. 2007;7:1811-22.

[20] Asadian-Birjand M, Sousa-Herves A, Steinhilber D, Cuggino JC, Calderon M. Functional nanogels for biomedical applications. Curr Med Chem. 2012;19:5029-43.

[21] Zhang X, Malhotra S, Molina M, Haag R. Micro- and nanogels with labile crosslinks - from synthesis to biomedical applications. Chem Soc Rev. 2015;44:1948-73.

[22] Molina M, Asadian-Birjand M, Balach J, Bergueiro J, Miceli E, Calderón M. Stimuli-responsive nanogel composites and their application in nanomedicine. Chemical Society Reviews. 2015;44:6161-86.

[23] Smith MH, Lyon LA. Multifunctional Nanogels for siRNA Delivery. Accounts of Chemical Research. 2012;45:985-93.

[24] Hellmund M, Zhou H, Samsonova O, Welker P, Kissel T, Haag R. Functionalized polyglycerol amine nanogels as nanocarriers for DNA. Macromol Biosci. 2014;14:1215-21.

[25] Zhang X, Achazi K, Steinhilber D, Kratz F, Dernedde J, Haag R. A facile approach for dual-responsive prodrug nanogels based on dendritic polyglycerols with minimal leaching. J Control Release. 2014;174:209-16.

[26] Kabanov AV, Vinogradov SV. Nanogels as pharmaceutical carriers: finite networks of infinite capabilities. Angew Chem Int Ed Engl. 2009;48:5418-29.

[27] Averick SE, Paredes E, Irastorza A, Shrivats AR, Srinivasan A, Siegwart DJ, et al. Preparation of Cationic Nanogels for Nucleic Acid Delivery. Biomacromolecules. 2012;13:3445-9.

[28] Blackburn WH, Dickerson EB, Smith MH, McDonald JF, Lyon LA. Peptide-Functionalized Nanogels for Targeted siRNA Delivery. Bioconjugate Chemistry. 2009;20:960-8.

[29] Raemdonck K, Naeye B, Buyens K, Vandenbroucke RE, Høgset A, Demeester J, et al. Biodegradable Dextran Nanogels for RNA Interference: Focusing on Endosomal Escape and Intracellular siRNA Delivery. Advanced Functional Materials. 2009;19:1406-15.

[30] Dunn SS, Tian S, Blake S, Wang J, Galloway AL, Murphy A, et al. Reductively Responsive siRNA-Conjugated Hydrogel Nanoparticles for Gene Silencing. Journal of the American Chemical Society. 2012;134:7423-30.

[31] Yang X-Z, Du J-Z, Dou S, Mao C-Q, Long H-Y, Wang J. Sheddable Ternary Nanoparticles for Tumor Acidity-Targeted siRNA Delivery. ACS Nano. 2012;6:771-81.

[32] Markovsky E, Baabur-Cohen H, Eldar-Boock A, Omer L, Tiram G, Ferber S, et al. Administration, distribution, metabolism and elimination of polymer therapeutics. J Control Release. 2012;161:446-60.

[33] Boussif O, Lezoualc'h F, Zanta MA, Mergny MD, Scherman D, Demeneix B, et al. A versatile vector for gene and oligonucleotide transfer into cells in culture and in vivo: polyethylenimine. Proc Natl Acad Sci U S A. 1995;92:7297-301.

[34] Bernardo PH, Brasch N, Chai CL, Waring P. A novel redox mechanism for the glutathione-dependent reversible uptake of a fungal toxin in cells. J Biol Chem. 2003;278:46549-55.

[35] Navarro J, Obrador E, Carretero J, Petschen I, Avino J, Perez P, et al. Changes in glutathione status and the antioxidant system in blood and in cancer cells associate with tumour growth in vivo. Free Radic Biol Med. 1999;26:410-8.

[36] Zhang X, Achazi K, Steinhilber D, Kratz F, Dernedde J, Haag R. A facile approach for dual-responsive prodrug nanogels based on dendritic polyglycerols with minimal leaching. Journal of Controlled Release. 2014;174:209-16.

[37] Merdan T, Callahan J, Petersen H, Kunath K, Bakowsky U, Kopeckova P, et al. Pegylated polyethylenimine-Fab' antibody fragment conjugates for targeted gene delivery to human ovarian carcinoma cells. Bioconjug Chem. 2003;14:989-96.

[38] Steinhilber D, Witting M, Zhang X, Staegemann M, Paulus F, Friess W, et al. Surfactant free preparation of biodegradable dendritic polyglycerol nanogels by inverse nanoprecipitation for encapsulation and release of pharmaceutical biomacromolecules. Journal of Controlled Release. 2013;169:289-95.

[39] Barnard A, Posocco P, Fermeglia M, Tschiche A, Calderon M, Pricl S, et al. Double-degradable responsive self-assembled multivalent arrays--temporary nanoscale recognition between dendrons and DNA. Org Biomol Chem. 2014;12:446-55.

[40] Malhotra S, Bauer H, Tschiche A, Staedtler AM, Mohr A, Calderon M, et al. Glycine-terminated dendritic amphiphiles for nonviral gene delivery. Biomacromolecules. 2012;13:3087-98.

[41] Barnard A, Posocco P, Pricl S, Calderon M, Haag R, Hwang ME, et al. Degradable self-assembling dendrons for gene delivery: experimental and theoretical insights into the barriers to cellular uptake. J Am Chem Soc. 2011;133:20288-300.

[42] Tschiche A, Malhotra S, Haag R. Nonviral gene delivery with dendritic self-assembling architectures. Nanomedicine (Lond). 2014;9:667-93.

[43] Sheikhi Mehrabadi F, Zeng H, Johnson M, Schlesener C, Guan Z, Haag R. Multivalent dendritic polyglycerolamine with arginine and histidine end groups for efficient siRNA transfection. Beilstein J Org Chem. 2015;11:763-72.

[44] Kelkar SS, Xue L, Turner SR, Reineke TM. Lanthanide-containing polycations for monitoring polyplex dynamics via lanthanide resonance energy transfer. Biomacromolecules. 2014;15:1612-24.

[45] Li D, Muller MB, Gilje S, Kaner RB, Wallace GG. Processable aqueous dispersions of graphene nanosheets. Nat Nanotechnol. 2008;3:101-5.

[46] Li N, Fu H, Tie Y, Hu Z, Kong W, Wu Y, et al. miR-34a inhibits migration and invasion by down-regulation of c-Met expression in human hepatocellular carcinoma cells. Cancer Lett. 2009;275:44-53.

[47] Sun F, Fu H, Liu Q, Tie Y, Zhu J, Xing R, et al. Downregulation of CCND1 and CDK6 by miR-34a induces cell cycle arrest. FEBS Lett. 2008;582:1564-8.

[48] Bu P, Chen KY, Chen JH, Wang L, Walters J, Shin YJ, et al. A microRNA miR-34a-regulated bimodal switch targets Notch in colon cancer stem cells. Cell Stem Cell. 2013;12:602-15.

[49] Yang F, Li QJ, Gong ZB, Zhou L, You N, Wang S, et al. MicroRNA-34a targets Bcl-2 and sensitizes human hepatocellular carcinoma cells to sorafenib treatment. Technol Cancer Res Treat. 2014;13:77-86.

[50] Li Y, Guessous F, Zhang Y, Dipierro C, Kefas B, Johnson E, et al. MicroRNA-34a inhibits glioblastoma growth by targeting multiple oncogenes. Cancer Res. 2009;69:7569-76.

[51] Moghimi SM, Szebeni J. Stealth liposomes and long circulating nanoparticles: critical issues in pharmacokinetics, opsonization and protein-binding properties. Prog Lipid Res. 2003;42:463-78.

[52] Simeoni F, Morris MC, Heitz F, Divita G. Peptide-based strategy for siRNA delivery into mammalian cells. Methods Mol Biol. 2005;309:251-60.

[53] Soutschek J, Akinc A, Bramlage B, Charisse K, Constien R, Donoghue M, et al. Therapeutic silencing of an endogenous gene by systemic administration of modified siRNAs. Nature. 2004;432:173-8.

[54] Ofek P, Fischer W, Calderon M, Haag R, Satchi-Fainaro R. In vivo delivery of small interfering RNA to tumors and their vasculature by novel dendritic nanocarriers. FASEB J. 2010;24:3122-34.

[55] Spagnou S, Miller AD, Keller M. Lipidic carriers of siRNA: differences in the formulation, cellular uptake, and delivery with plasmid DNA. Biochemistry. 2004;43:13348-56.

[56] Duncan R. Polymer conjugates for tumour targeting and intracytoplasmic delivery. The EPR effect as a common gateway? Pharm Sci Technolo Today. 1999;2:441-9.

[57] Scomparin A, Polyak D, Krivitsky A, Satchi-Fainaro R. Achieving successful delivery of oligonucleotides--From physico-chemical characterization to in vivo evaluation. Biotechnol Adv. 2015;33:1294-309.

[58] Gao Y, Xie J, Chen H, Gu S, Zhao R, Shao J, et al. Nanotechnology-based intelligent drug design for cancer metastasis treatment. Biotechnol Adv. 2014;32:761-77.

[59] Gratton SE, Ropp PA, Pohlhaus PD, Luft JC, Madden VJ, Napier ME, et al. The effect of particle design on cellular internalization pathways. Proc Natl Acad Sci U S A. 2008;105:11613-8.

[60] Miller CR, Bondurant B, McLean SD, McGovern KA, O'Brien DF. Liposome-cell interactions in vitro: effect of liposome surface charge on the binding and endocytosis of conventional and sterically stabilized liposomes. Biochemistry. 1998;37:12875-83.

[61] Elouahabi A, Ruysschaert JM. Formation and intracellular trafficking of lipoplexes and polyplexes. Mol Ther. 2005;11:336-47.